Chapter 3

Difference synchronization among three chaotic systems with exponential term and its chaos control

3.1 Introduction

The synchronization phenomenon and chaos control of dynamical systems are very important topics in science and engineering from the philosophical and practical points of view. In synchronization, the master and the slave systems are coupled by using control technique, and it expresses an idea of strong correlations between coupled systems.

Synchronization is the basic term to understand the natural phenomenon in details, and it exists in nature from cosmology and natural rhythms like heart beating (Strogatz (2003)) and handclapping (Néda et al. (2000)) to superconductors (Wiesenfeld et al. (1996)). In medical synchronization, it is often beneficial for us, some pathologies of the brain such as Parkinson disease (Tass et al. (1998), Hammond et al. (2007)) and epilepsy (Garcia et al. (2005)), which are also related to this synchronization phenomena. Synchronization is also found in engineering and technology specially in laser synchronize (Winful and Rahman (1990), Oliva and Strogatz (2001), Hirosawa et al. (2013)), synchronization between the bridges' oscillations and pedestrians' gait (Eckhardt et al. (2007), Strogatz et al. (2005), Belykh et al. (2016)).

Synchronization is used effectively to create secure communication schemes (Kocarev and Parlitz (1995), Stankovski et al. (2014), Ren et al. (2013), Eroglu et al. (2017), Koronovskii et al. (2009)) and it can help in developing innovative technologies. Synchronization is also used for model calibration (Parlitz (1996), Yu and Parlitz (2008)).

The contents of this chapter have been published in ***Chaos, Solitons & Fractals, 124, 36-51, 2019***.

In the twentieth century, the chaos in dynamics was scientific revolution. It is related to our understanding of the nature of unpredictability. In the late nineteenth century, it was initiated by Henri Poincaré, and chaos revolution took off in the 1980's after the invention of highly configured computers. A positive maximum Lyapunov exponent measures the chaos, and it arises when recurrent dynamical behavior has locally dispersing characteristics.

Recently, many types of chaos synchronization schemes have been developed by researchers including the generalized synchronization (Wu et al. (2012), Yang et al. (1998), Ghosh et al. (2018)), complete synchronization (Pecora and Carroll (1990), Carroll and Pecora (1997)), phase and anti-phase synchronization (Rosenblum et al. (1996), Yadav et al. (2017)), lag synchronization (Xia (2009)), combination synchronization (Runzi et al. (2011), Yadav et al. (2017)), combination-combination synchronization (Sun et al. (2013)), compound synchronization (Sun et al. (2013)), double compound synchronization (Zhang and Deng (2014)) etc. and it is also necessary to develop different types of complicated chaos synchronization processes in order to reduce the chances of hacking. The new type of chaos synchronization scheme becomes uncertain for understanding to cybercriminals, and as a result, it is difficult to hack the transmitted information. The new type of synchronization such as difference synchronization is achieved in three systems with the exponential terms consisting of two drive and one response systems, and the realization of difference synchronization has increased the existing number of varieties of chaos schemes.

To achieve the above types of synchronization scheme, several synchronization methods have been developed such as linear and nonlinear feedback method (Li et al. (2009)), active control method (Agrawal et al. (2012)), adaptive control method (Liao and Tsai

(2000)), OGY method (Ott et al. (1990)), sliding mode control method (Cai et al. (2010)), backstepping method (Li et al. (2006), Das and Yadav (2016)) etc. Among these methods, the linear feedback control is used during chaos control and difference synchronization, and it is found that this method is most powerful and suitable for chaos control and synchronization of chaotic systems with exponential terms.

The literature survey is revealing that the nonlinear dynamics is an attractive field which has been extensively studied during the last few decades. A chaotic system is another type of dynamical system which is very sensitive to its initial conditions. Firstly, in 1990, Pecora and Carroll (1990) had proposed the concept of synchronization in chaotic systems. Same time, Vaidya et al. (1990) have visualized the synchronization of two identical chaotic systems with virtually identical initial conditions. Chen and Lü (2002) used the adaptive control method in the study of synchronization of an uncertain unified chaotic system. Chaos synchronization between each pair of Lorenz, Lü and Chen systems have been analyzed by Yassen (2005). Mainieri and Rehacek (1999) have studied projective synchronization in three dimensional chaotic systems for the Lorenz and disk dynamo systems. Synchronization of Genesio chaotic system was visualized by Park (2006) applying the adaptive back-stepping approach in the derivation of the error signals between identical Genesio systems. Blasius et al. (1990) also analyzed complex dynamics and phase synchronization in ecological systems. Huang et al. (2004) used non-linear control method to synchronize two identical and two different chaotic systems. To analyze their results, they considered Lü system as identical systems, and Lur'e-like and Genesio systems for different chaotic systems. Xiao and Dayong (2014) have studied a five-dimensional system and used nonlinear feedback and anti-synchronization approach. Zhang and Deng (2014) have investigated a novel type of synchronization by four master systems and two slave systems. This synchronization is equivalent to two compound synchronization, which is the so-called double compound synchronization. Lightbody and Irwin (1997) analyzed applications of the neural network model in plant modeling and developed internal model control. Runzi and Yinglan (2012) studied combination synchronization of three different chaotic systems. In 2014, Ahmed et al. (2014) have introduced, the exponential nonlinear term with Chen's attractor and discussed several features of this new attractors. Pham et al. (2015) developed a new chaotic system with the addition of exponential nonlinear term and showed that this system exhibits the behavior of hidden attractors and having no equilibrium points. Cheng et al. (2018) discussed a new type of robust chaotic system with the exponential, quadratic term and explained that this system exhibits periodic and chaotic behaviors. Deng et al. (2017) used an exponential term in the investigation of a different type of chaotic system. Yu and Wang (2012) discussed a novel three-dimensional chaotic system with a quadratic, exponential nonlinear term and studied several basic dynamical properties. Motivated by above studies, in this article, the authors have studied difference synchronization among Ten ring chaotic system, 3D chaotic system and new 3D chaotic system in the presence of exponential terms and also studied the chaos control of these systems using feedback control technique. The difference synchronization scheme is used in chaotic secure communication to enhance security information.

The organization of the chapter is as follows: In section 3.1, the introduction is given. In section 3.2, the difference synchronization scheme is introduced, and section 3 contains the Routh-Hurwitz Criterion. In section 3.4, the systems' descriptions and chaos control of the Ten rings chaotic system, 3D chaotic system, new 3D chaotic system are explained. In section 3.5, the difference synchronization scheme is applied for the cases of three continuous and three discrete time chaotic systems. In section 3.6, the numerical simulation of the difference synchronization scheme is discussed, which is followed by the section with conclusion of the overall work.

3.2 Difference synchronization scheme

For difference synchronization, we consider the two master systems and one slave system.

The two master systems are considered as

$$\frac{dX_1}{dt} = A_1 X_1 + F_1(X_1), \tag{3.1}$$

$$\frac{dX_2}{dt} = A_2 X_2 + F_2(X_2), \tag{3.2}$$

and the slave system is taken as

$$\frac{dX_3}{dt} = A_3 X_3 + F_3(X_3) + U(X_1, X_2, X_3), \tag{3.3}$$

where $X_1 = [x_{11}(t), x_{12}(t), ..., x_{1n}(t)]^T$, $X_2 = [x_{21}(t), x_{22}(t), ..., x_{2n}(t)]^T$, $X_3 = [x_{31}(t), x_{32}(t), ..., x_{3n}(t)]^T$ are state vectors of master systems (3.1), (3.2) and slave system (3.3), $F_1, F_2, F_3 : R^n \to R^n$ are the continuous vector functions and $U(X_1, X_2, X_3) : R^n \times R^n \times R^n \to R^n$ is a controller and it will be designed later using control technique.

Definition 3.1: The master systems (3.1), (3.2) and slave system (3.3) are said to be difference synchronized if

$$\lim_{t\to\infty} \|L_3 X_3 - (L_2 X_2 - L_1 X_1)\| = 0,$$

where $L_3 = diag(l_{31}, l_{32}, l_{33}) \neq 0$, $L_2 = diag(l_{21}, l_{22}, l_{23})$ and $L_1 = diag(l_{11}, l_{12}, l_{13})$ are three constant matrices and $\| \ \|$ denotes the norm of the matrix.

Remark I: If we consider the constant matrices as $L_3 \neq 0$, $L_2 = 0$ and $L_1 \neq 0$, then the difference synchronization problem is reduced to the anti-synchronization problem.

Remark II: Considering the constant matrices as $L_3 \neq 0$, $L_2 \neq 0$ and $L_1 = 0$, the difference synchronization problem is reduced to the synchronization problem.

Remark III: Considering the constant matrices as $L_3 \neq 0$, $L_2 = 0$ and $L_1 = 0$, the difference synchronization problem is reduced to the chaos control problem.

3.3 Routh-Hurwitz Criterion

Let us consider the *n*-th order homogeneous system of differential equations with constant coefficient as

$$\frac{dX(t)}{dt} = AX(t), \tag{3.4}$$

where $X = [x_1(t),\, x_2(t), \ldots, x_n(t)]^T$ is the n-dimensional vector containing the unknown function and $A = \begin{bmatrix} a_{11} & a_{12} & \cdots & a_{1n} \\ a_{21} & a_{22} & \cdots & a_{2n} \\ \cdots & \cdots & \cdots & \cdots \\ a_{n1} & a_{n2} & \cdots & a_{nn} \end{bmatrix}$ is a square matrix of size $n \times n$.

The stability of the equilibrium point is determined by the sign of the real parts of the eigenvalues of the matrix *A*, and to find the eigenvalues, it is necessary to solve the following characteristic equation

$$\det(A - \lambda I) = 0, \tag{3.5}$$

which gives an algebraic equation as

$$a_0\lambda^n + a_1\lambda^{n-1} + a_2\lambda^{n-2} + \ldots + a_{n-1}\lambda + a_n = 0, \tag{3.6}$$

which describes the dynamic system.

Let, $$H = \begin{bmatrix} a_1 & a_0 & 0 & 0 & 0 & 0 & \dots & 0 \\ a_3 & a_2 & a_1 & a_0 & 0 & 0 & \dots & 0 \\ a_5 & a_4 & a_3 & a_2 & a_1 & a_0 & \dots & 0 \\ \dots & \dots & \dots & \dots & \dots & \dots & \dots & \dots \\ 0 & 0 & 0 & 0 & 0 & 0 & \dots & a_n \end{bmatrix} \quad (3.7)$$

be the Hurwitz matrix of the polynomial (3.6), and the roots of the auxiliary equation (3.5) have negative real parts if and only if the principal diagonal minors Δ_i of the Hurwitz matrix (3.7) are all positive, *i.e.*, $\Delta_1 > 0$, $\Delta_2 > 0$, ..., $\Delta_n > 0$,

where $\Delta_1 = |a_1|$, $\Delta_2 = \begin{vmatrix} a_1 & a_0 \\ a_3 & a_2 \end{vmatrix}$, $\Delta_3 = \begin{vmatrix} a_1 & a_0 & 0 \\ a_3 & a_2 & a_1 \\ a_5 & a_4 & a_3 \end{vmatrix}$, ..., $\Delta_n = \begin{vmatrix} a_1 & a_0 & 0 & \dots & 0 \\ a_3 & a_2 & a_1 & \dots & 0 \\ a_5 & a_4 & a_3 & \dots & 0 \\ \dots & \dots & \dots & \dots & \dots \\ 0 & 0 & 0 & \dots & a_n \end{vmatrix}$

and hence the system will be stabilized.

The Routh-Hurwitz stability condition for 2^{nd}, 3^{rd} and 4^{th} order systems are defined as

(i) $a_0\lambda^2 + a_1\lambda + a_2 = 0$,

the stability criterion is satisfied by the inequalities

$$\Delta_1 = a_1 > 0,\ \Delta_2 = \begin{vmatrix} a_1 & a_0 \\ a_3 & a_2 \end{vmatrix} = a_1 a_2 > 0, \text{ since } a_3 = 0.$$

(ii) $a_0\lambda^3 + a_1\lambda^2 + a_2\lambda + a_3 = 0.$

Here the stability criterion satisfied by the following inequalities

$$\Delta_1 = a_1 > 0,\ \Delta_2 = \begin{vmatrix} a_1 & a_0 \\ a_3 & a_2 \end{vmatrix} = a_1 a_2 - a_0 a_3 > 0,\ \Delta_3 = a_3 > 0.$$

(iii) $a_0\lambda^4 + a_1\lambda^3 + a_2\lambda^2 + a_3\lambda + a_4 = 0$, for the stability criterion to be satisfied, the inequalities will be

$$\Delta_1 = a_1 > 0,\ \Delta_2 = \begin{vmatrix} a_1 & a_0 \\ a_3 & a_2 \end{vmatrix} = a_1 a_2 - a_0 a_3 > 0,$$

$$\Delta_3 = \begin{vmatrix} a_1 & a_0 & 0 \\ a_3 & a_2 & a_1 \\ 0 & a_4 & a_3 \end{vmatrix} = a_1 a_2 a_3 - a_1^2 a_4 - a_0 a_3^2 > 0,\ \Delta_4 = a_4 > 0.$$

Hence all the roots of 2nd, 3rd and 4th order polynomials have negative real parts when the above inequalities hold. Hence the considered system (3.4) will be stable.

3.4 Systems' descriptions and control of chaos

3.4.1 Ten-ring chaotic system

The Ten-ring chaotic continuous-time three-dimensional autonomous system (Deng et al. (2017)) is defined as

$$\frac{dx_{11}}{dt} = a_{11}(x_{11} + x_{12}),$$

$$\frac{dx_{12}}{dt} = -a_{13}x_{12} - x_{11}x_{13} + a_{14}x_{11}, \tag{3.8}$$

$$\frac{dx_{13}}{dt} = -a_{12}x_{13} + e^{x_{11}^2},$$

where x_{11}, x_{12}, x_{13} are the state variables, a_{11}, a_{12}, a_{13} and a_{14} are the positive constant parameters. The system (3.8) shows chaotic behavior for the parameters' values $a_{11} = 20$, $a_{12} = 2$, $a_{13} = 28$, $a_{14} = 0.5$ with the initial condition $(0.02, 0.01, 0.03)$ which is depicted through Fig. 3.1.

Taking the first approximation of the exponential term $e^{x_{11}^2}$ of equation (3.8), the Ten-ring chaotic system reduces to a classical chaotic system which also shows the chaotic behavior with the same values of parameters and initial condition whose phase portraits are depicted through Fig. 3.2.

As $\nabla.V = \frac{\partial \dot{x}_{11}}{\partial x_{11}} + \frac{\partial \dot{x}_{12}}{\partial x_{12}} + \frac{\partial \dot{x}_{13}}{\partial x_{13}} = a_{11} - a_{13} - a_{12} = -10 < 0$, the system (3.8) is a dissipative system, and the solution of the system will be bounded as time approaches to infinity. The system is symmetrical under the coordinate transformation $(-x_{11}, -x_{12}, x_{13}) \to (x_{11}, x_{12}, x_{13})$ i.e., the system has rotation symmetry around x_{13}-axis. The system (3.8) has three Lyapunov exponents with the same initial condition and parametric values as 0.8196, -0.0110, −10.8079. Thus the system (3.8) is chaotic. Since the considered system is dissipative system therefore even we calculate the values of the maximum Lyapunov exponents in the close points to the said initial condition, we cannot find much differences as seen from Table 3.1. The calculations of Lyapunov exponents are made through Matlab software using Algorthim-1 proposed by Wolf et. al. (1985), which was later used by Singh and Roy (2016).

Now the equilibrium points of the Ten ring system (3.8) will be obtained by solving the following equations

$a_{11}(x_{11} + x_{12}) = 0$, $-a_{13}x_{12} - x_{11}x_{13} + a_{14}x_{11} = 0$, $-a_{12}x_{13} + e^{x_{11}^2} = 0$.

The system (3.8) has three equilibrium points as $E_{11} = (0, 0, \frac{1}{a_{12}})$, $E_{12} = (\sqrt{\log(a_{12}a_{13} + a_{12}a_{14})}, -\sqrt{\log(a_{12}a_{13} + a_{12}a_{14})}, a_{13} + a_{14})$, $E_{13} = (-\sqrt{\log(a_{12}a_{13} + a_{12}a_{14})}, \sqrt{\log(a_{12}a_{13} + a_{12}a_{14})}, a_{13} + a_{14})$. After putting the values of parameters the equilibrium points give the numeric form as $E_{11} = (0, 0, 0.5)$, $E_{12} = (2.01073, -2.01073, 28.50)$, $E_{13} = (-2.01073, 2.01073, 28.50)$.

Table 3.1 Lyapunov exponents for the Ten-ring chaotic system for the parameters' values $a_{11} = 20$, $a_{12} = 2$, $a_{13} = 28$, $a_{14} = 0.5$

Sl. No.	Initial Condition	Observation Time (T)	Lyapunov Exponents
1	2, 0, 3	10000	0.8060, -0.0143, -10.7906
2	1, 4, 2	10000	0.7652, -0.0152, -10.7490
3	3, 2, 4	10000	0.7972, -0.0124, -10.7838
4	-0.3, -1, -2.5	10000	0.7822, -0.0093, -10.7719

3.4.1.1 Control of chaos

For chaos control defining the ten chaotic systems with control functions as

$$\frac{dx_{11}}{dt} = a_{11}(x_{11} + x_{12}) + u_{11}(t),$$

$$\frac{dx_{12}}{dt} = -a_{13}x_{12} - x_{11}x_{13} + a_{14}x_{11} + u_{12}(t), \tag{3.9}$$

$$\frac{dx_{13}}{dt} = -a_{12}x_{13} + e^{x_{11}^2} + u_{13}(t),$$

where $u_{11}(t) = k_{11}(x_{11} - \bar{x}_{11})$, $u_{12}(t) = k_{12}(x_{12} - \bar{x}_{12})$ and $u_{13}(t) = k_{13}(x_{13} - \bar{x}_{13})$ are the control functions. After substituting these values in equation (3.9), we

$$\frac{dx_{11}}{dt} = a_{11}(x_{11} + x_{12}) + k_{11}(x_{11} - \bar{x}_{11}),$$

$$\frac{dx_{12}}{dt} = -a_{13}x_{12} - x_{11}x_{13} + a_{14}x_{11} + k_{12}(x_{12} - \bar{x}_{12}), \tag{3.10}$$

$$\frac{dx_{13}}{dt} = -a_{12}x_{13} + e^{x_{11}^2} + k_{13}(x_{13} - \bar{x}_{13}),$$

where k_{11}, k_{12} and k_{13} are the feedback controllers, which are chosen in such a way that the trajectory of the system will be stabilized to any of the above three equilibrium points.

At the equilibrium point $\overline{E}_1 = (\overline{x}_{11}, \overline{x}_{12}, \overline{x}_{13})$, the Jacobian matrix of the system (3.10) is obtained as

$$J_1(\overline{E}_1) = \begin{bmatrix} (a_{11}+k_{11}) & a_{11} & 0 \\ -\overline{x}_{13}+a_{14} & -a_{13}+k_{12} & -\overline{x}_{11} \\ 2\overline{x}_{11}e^{\overline{x}_{11}^2} & 0 & -a_{12}+k_{13} \end{bmatrix}. \quad (3.11)$$

Lemma 3.1: The equilibrium point $E_{11} = (0, 0, \frac{1}{a_{12}})$ of the controlled system (3.10) is asymptotically stable if $k_{11} < -a_{11}$, $k_{12} < a_{13}$, $k_{13} < a_{12}$.

Proof: From equation (3.11), the Jacobian matrix of the system (3.10) at the equilibrium point E_{11} will be

$$J_{11}(E_{11}) = \begin{bmatrix} (a_{11}+k_{11}) & a_{11} & 0 \\ 0 & -a_{13}+k_{12} & 0 \\ 0 & 0 & -a_{12}+k_{13} \end{bmatrix}. \quad (3.12)$$

The eigenvalues of the Jacobian matrix (3.12) are $\lambda_1 = a_{11}+k_{11}$, $\lambda_2 = -a_{13}+k_{12}$ and $\lambda_3 = -a_{12}+k_{13}$, where a_{11}, a_{12}, a_{13} are the constant parameters of the system (3.8); therefore the equilibrium point E_{11} of the system (3.8) will be asymptotically stable if $k_{11} < -a_{11}$, $k_{12} < a_{13}$, $k_{13} < a_{12}$. The plots of the trajectories are depicted in Fig. 3.3(a).

Lemma 3.2: The equilibrium point $E_{12}(\sqrt{\log(a_{12}a_{13}+a_{12}a_{14})}, -\sqrt{\log(a_{12}a_{13}+a_{12}a_{14})}, a_{13}+a_{14})$ or $E_{12}(p, -p, r)$, where $p = \sqrt{\log(a_{12}a_{13}+a_{12}a_{14})}$ and $r = a_{13}+a_{14}$ of the controlled system (3.10) is asymptotically stable if $k_{11} < -a_{11}$, $k_{12} < 0$, $k_{13} < 0$.

Proof: The Jacobian matrix of the controlled system (3.10) at the equilibrium point E_{12} is

$$J_{12}(E_{12})=\begin{bmatrix}(a_{11}+k_{11}) & a_{11} & 0 \\ -r+a_{14} & -a_{13}+k_{12} & -p \\ 2pe^{p^2} & 0 & -a_{12}+k_{13}\end{bmatrix}. \tag{3.13}$$

The characteristic polynomial of the Jacobian matrix (3.13) is

$$\lambda^3-(k_{13}-a_{12}-a_{13}+k_{12}+a_{11}+k_{11})\lambda^2-[(k_{13}-a_{12})(a_{13}-k_{12}-a_{11}-k_{11})-a_{11}(r-a_{14})$$
$$+(a_{11}+k_{11})(a_{13}-k_{12})]\lambda+2a_{11}e^{p^2}p^2-(k_{13}-a_{12})[a_{11}(r-a_{14})-(a_{11}+k_{11})(a_{13}-k_{12})]=0$$

If we consider $a_1=-(k_{13}-a_{12}-a_{13}+k_{12}+a_{11}+k_{11})$, $a_2-(k_{13}-a_{12})(a_{13}-k_{12}-a_{11}-k_{11})+a_{11}(r-a_{14})-(a_{11}+k_{11})(a_{13}-k_{12})$, and $a_3=2a_{11}e^{p^2}p^2-(k_{13}-a_{12})[a_{11}(r-a_{14})-(a_{11}+k_{11})(a_{13}-k_{12})]$, then characteristic polynomial is reduced to the following form

$$\lambda^3+a_1\lambda^2+a_2\lambda+a_3=0.$$

In the view of the Routh-Hurwitz condition (ii), if we consider $k_{11}<-a_{11}$, $k_{12}<0$, $k_{13}<0$, the controlled system (3.10) will be asymptotically stable at the point E_{12}.

Similarly, the equilibrium point $E_{13}=(-\sqrt{\log(a_{12}a_{13}+a_{12}a_{14})},\sqrt{\log(a_{12}a_{13}+a_{12}a_{14})},a_{13}+a_{14})$ or $E_{13}=(-p,p,r)$ of the system (3.10) is asymptotically stable if we choose the feedback controllers as $k_{11}<-a_{11}$, $k_{12}<0$, $k_{13}<0$.

The unstable trajectories of Ten-ring chaotic system are controlled at its equilibrium points, and the plots of trajectories of the system are given in Figs. 3.3(a)-(c).

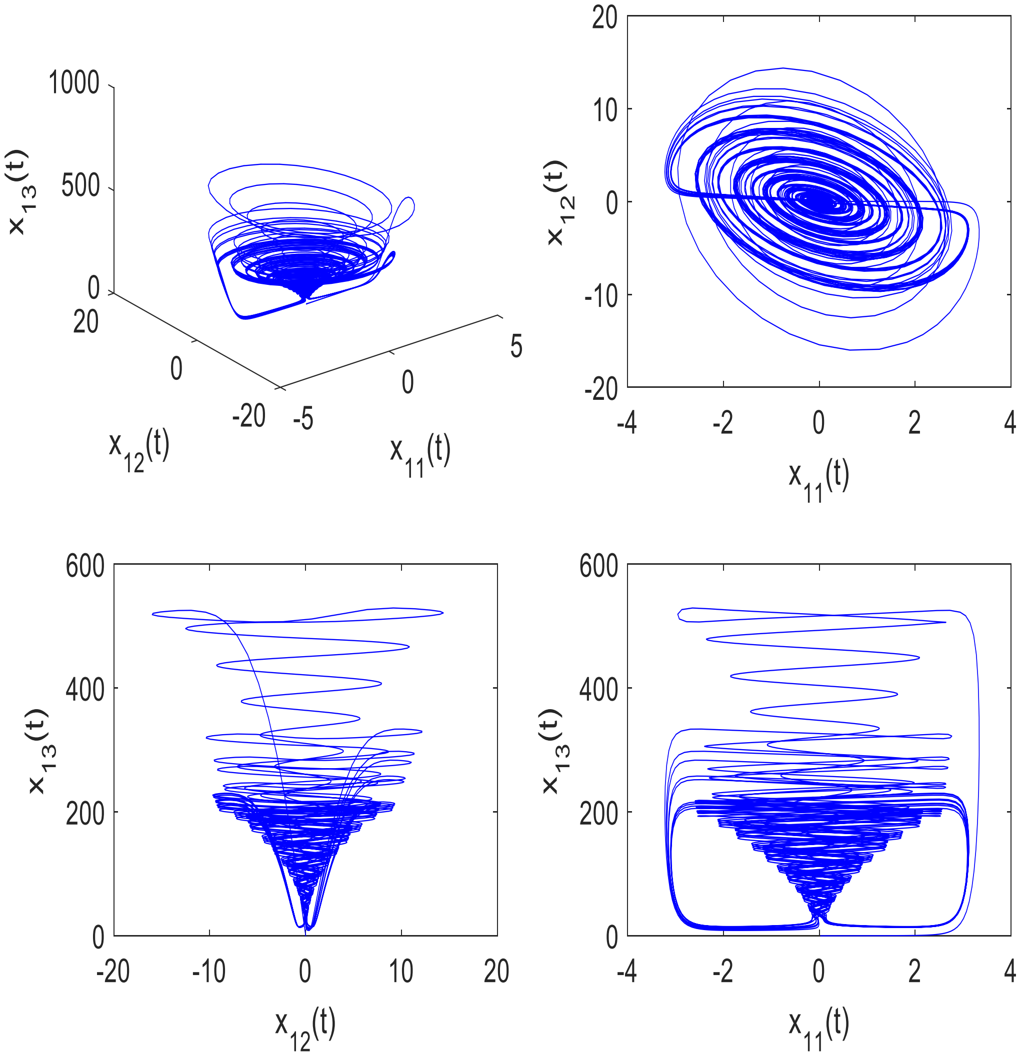

Fig. 3.1 Chaotic attractors of Ten-ring chaotic system with exponential term for the values of the parameters $a_{11}=20$, $a_{12}=2$, $a_{13}=28$, $a_{14}=0.5$ and initial condition $(0.02, 0.01, 0.03)$.

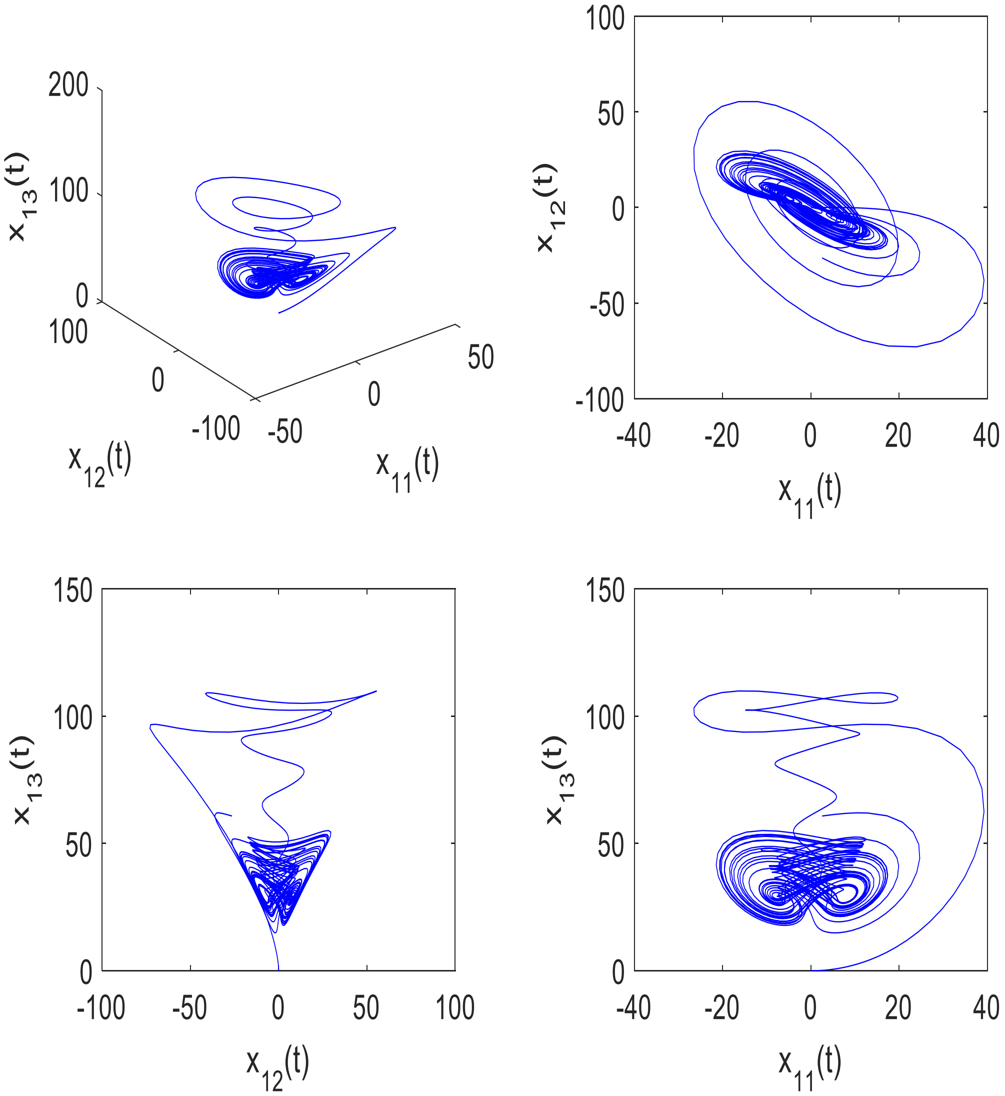

Fig. 3.2 Chaotic attractors of Ten-ring chaotic system without exponential term for the values of the parameters $a_{11}=20$, $a_{12}=2$, $a_{13}=28$, $a_{14}=0.5$ and initial condition $(0.02, 0.01, 0.03)$.

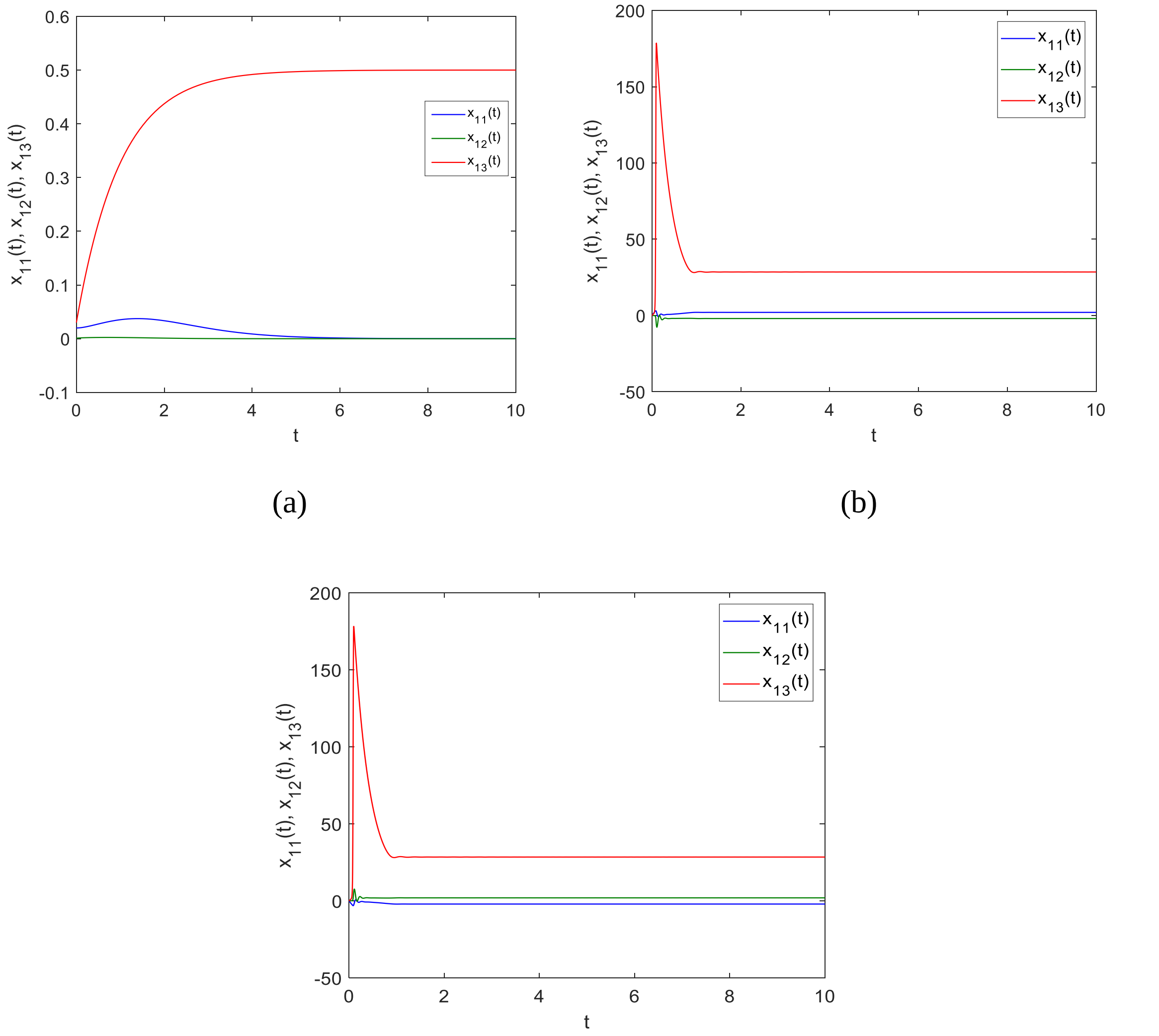

(a) (b)

(c)

Fig. 3.3 Chaos control of Ten-ring chaotic system (a) at the equilibrium point E_{11}, (b) at the equilibrium point E_{12}, (c) at the equilibrium point E_{13}.

3.4.2 3D chaotic system

The 3D chaotic system (Pham et al. (2015)) is defined as

$$\frac{dx_{21}}{dt} = a_{21}(x_{22} - x_{21}),$$

$$\frac{dx_{22}}{dt} = -a_{22}x_{22} + kx_{21}x_{23}, \tag{3.14}$$

$$\frac{dx_{23}}{dt} = a_{23} - e^{x_{21}x_{22}},$$

where the x_{21}, x_{22}, x_{23} are the state variables and a_{21}, a_{22}, a_{23}, k are the constant parameters. The system has chaotic behavior if we take the parametric values as $a_{21} = 0.8696$, $a_{22} = 0.5$, $a_{23} = 10.5$, $k = 0.756144$ and initial condition as $(x_{21}, x_{22}, x_{23}) = (-0.08, -1.02, -0.49)$. It displays a double-scroll chaotic attractor which are shown through Fig. 3.4. The system (3.14) has three Lyapunov exponents as 0.4936, 0, -1.8632 and thus the system is chaotic. Table 3.2 shows that the Lyapunov exponent will not be changed much even close points to initial condition due to the dissipative nature of the system.

The 3D chaotic system with exponential term is reduced to a classical chaotic system if we take the term $x_{21}x_{22}$ in the place of exponential term $e^{x_{21}x_{22}}$ of equation (3.14), and the system also shows the chaotic behavior with the same parametric values and the plots of the chaotic attractors are depicted through Fig. 3.5.

It is easy to verify that the system is invariant under the coordinate transformation $(x_{21}, x_{22}, x_{23}) \rightarrow (-x_{21}, -x_{22}, x_{23})$ i.e., the system has rotation symmetry around the x_{23}-axis. For system (3.14), the divergence $\nabla.V = -(a_{21} + a_{22}) < 0$ and thus the system (3.14) is dissipative with $(a_{21} + a_{22}) > 0$, and the solutions of the system are bounded with time.

To find equilibrium points, we solve the following system of equations,

$a_{21}(x_{22} - x_{21}) = 0, \ -a_{22}x_{22} + kx_{21}x_{23} = 0, \ a_{23} - e^{x_{21}x_{22}} = 0.$

If $a_{23} < 1$ or $a_{23} \neq 1$ and $k = 0$, the system (3.14) has no equilibrium points. If $a_{23} = 1$, the system has all equilibrium points in the form $(0, 0, n), n \in R$ and it will be non-isolated if $a_{23} > 1$, $k \neq 0$. The system has two equilibrium points as

$E_{21} = (-\sqrt{\log(a_{23})},\ -\sqrt{\log(a_{23})},\ \frac{a_{22}}{k}),$ $E_{22} = (\sqrt{\log(a_{23})},\ \sqrt{\log(a_{23})},\ \frac{a_{22}}{k}),$ or

$E_{21} = (-1.53342,\ -1.53342,\ 0.66125)$, $E_{22} = (1.53342, 1.53342,\ 0.66125)$.

Table 3.2 Lyapunov exponents for the 3D chaotic system for the parameters' values $a_{21} = 0.8696$, $a_{22} = 0.5$, $a_{23} = 10.5$, $k = 0.756144$

Sl. No.	Initial Condition	Observation Time(T)	Lyapunov Exponents
1	1, 0, -0.5	10000	0.4929, 0.0004, -1.8629
2	1, 4, 2	10000	0.4853, 0.0001, -1.8551
3	3, 1, 5	10000	0.4922, 0.0003, -1.8621
4	-2, -1, -3	10000	0.4887, 0.0001, -1.8585

3.4.2.1 Control of chaos

Consider the 3D chaotic system with control function as

$$\frac{dx_{21}}{dt} = a_{21}(x_{22} - x_{21}) + u_{21}(t),$$

$$\frac{dx_{22}}{dt} = -a_{22}x_{22} + kx_{21}x_{23} + u_{22}(t), \qquad (3.15)$$

$$\frac{dx_{23}}{dt} = a_{23} - e^{x_{21}x_{22}} + u_{23}(t),$$

where $u_{21}(t) = k_{21}(x_{21} - \bar{x}_{21})$, $u_{22}(t) = k_{22}(x_{22} - \bar{x}_{22})$, $u_{23}(t) = k_{23}(x_{23} - \bar{x}_{23})$ are control functions and k_{21}, k_{22}, k_{23} are the feedback controllers. Hence the controlled system (3.15) is rewritten as

$$\frac{dx_{21}}{dt} = a_{21}(x_{22} - x_{21}) + k_{21}(x_{21} - \bar{x}_{21}),$$

$$\frac{dx_{22}}{dt} = -a_{22}x_{22} + kx_{21}x_{23} + k_{22}(x_{22} - \bar{x}_{22}), \qquad (3.16)$$

$$\frac{dx_{23}}{dt} = a_{23} - e^{x_{21}x_{22}} + k_{23}(x_{23} - \bar{x}_{23}).$$

The Jacobian matrix of the system (3.16) at the equilibrium point $E_2 = (\bar{x}_{21}, \bar{x}_{22}, \bar{x}_{23})$ is given as

$$J_2(E_2) = \begin{bmatrix} -a_{21} + k_{21} & a_{21} & 0 \\ k\bar{x}_{23} & -a_{22} + k_{22} & k\bar{x}_{21} \\ -\bar{x}_{22}e^{\bar{x}_{21}\bar{x}_{22}} & -\bar{x}_{21}e^{\bar{x}_{21}\bar{x}_{22}} & k_{23} \end{bmatrix}. \quad (3.17)$$

Lemma 3.3: The equilibrium point $E_{21} = (-\sqrt{\log(a_{23})}, -\sqrt{\log(a_{23})}, \frac{a_{22}}{k})$ or $E_{21} = (-p_1, -p_1, r_1)$, where $p_1 = \sqrt{\log(a_{23})}$, $r_1 = \frac{a_{22}}{k}$ of the controlled system (3.16) will be asymptotically stable if $k_{21} < 0$, $k_{22} < 0$, $k_{23} < 0$.

Proof: At the equilibrium point $E_{21} = (-p_1, -p_1, r_1)$, the Jacobian matrix is

$$J_{21}(E_{21}) = \begin{bmatrix} -a_{21} + k_{21} & a_{21} & 0 \\ kr_1 & -a_{22} + k_{22} & -kp_1 \\ p_1e^{p_1^2} & p_1e^{p_1^2} & k_{23} \end{bmatrix}. \quad (3.18)$$

The characteristic polynomial of the Jacobian matrix (3.18) is

$$\lambda^3 + a_1\lambda^2 + a_2\lambda + a_3 = 0,$$

where $a_1 = a_{21} + a_{22} - k_{21} - k_{22} - k_{23}$,

$a_2 = -a_{21}kr_1 - (a_{21} - k_{21})(a_{22} - k_{22}) - k_{23}(a_{21} + a_{22} - k_{21} - k_{22}) + e^{p_1^2}p_1^2k$ and

$a_3 = -k_{23}\{(a_{21} - k_{21})(a_{22} - k_{22}) - kp_1^2(e^{p_1^2}k_{21} - 2a_{21}e^{p_1^2})\}$.

Now, from Routh-Hurwitz condition (ii), if we take $k_{21} < 0$, $k_{22} < 0$, $k_{23} < 0$, the controlled system (3.16) will be asymptotically stable at the point E_{21}.

Similarly, the equilibrium point $E_{22}=(\sqrt{\log(a_{23})},\ \sqrt{\log(a_{23})},\ \frac{a_{22}}{k})$ or $E_{22}=(p_1,\ p_1,\ r_1)$ of the system (3.14) is asymptotically stable if we consider similar feedback controllers. The plots of stable trajectories of 3D controlled system at its equilibrium points are shown in Figs. 3.6(a)-(b).

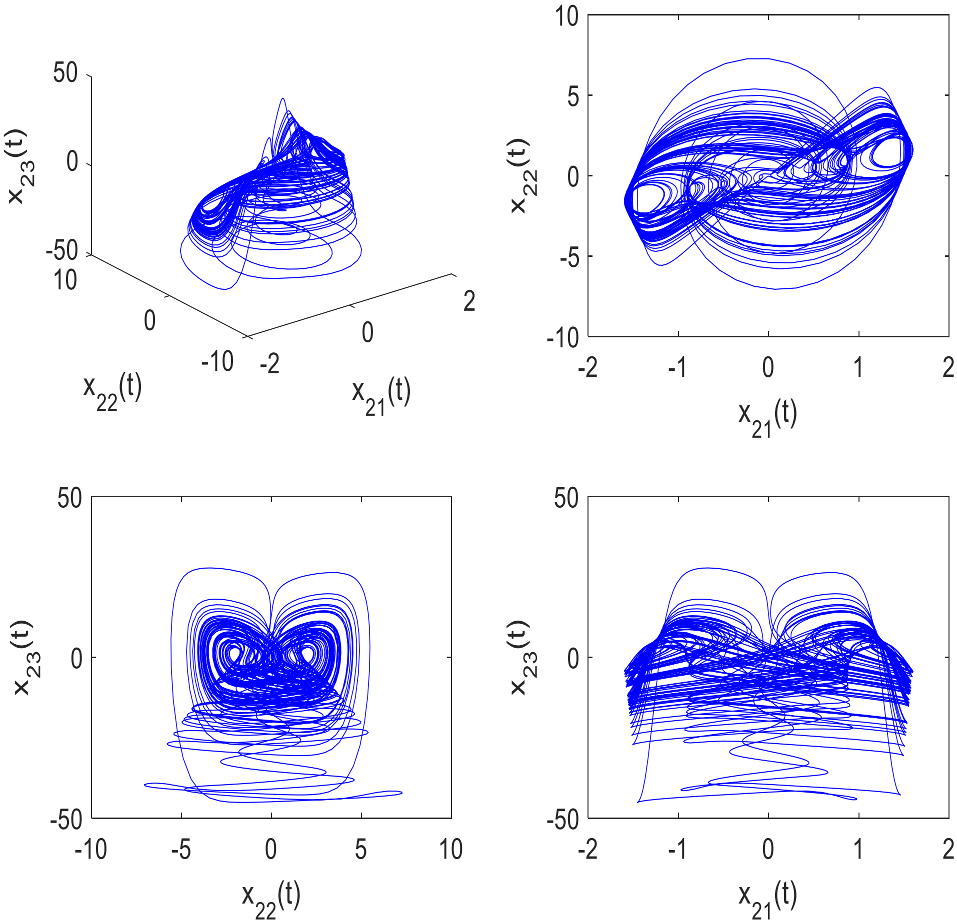

Fig. 3.4 Chaotic attractors of 3D chaotic system with exponential term for the values of the parameters $a_{21}=0.8696$, $a_{22}=0.5$, $a_{23}=10.5$, $k=0.756144$ and initial condition $(x_{21}, x_{22}, x_{23})=(-0.08, -1.02, -0.49)$.

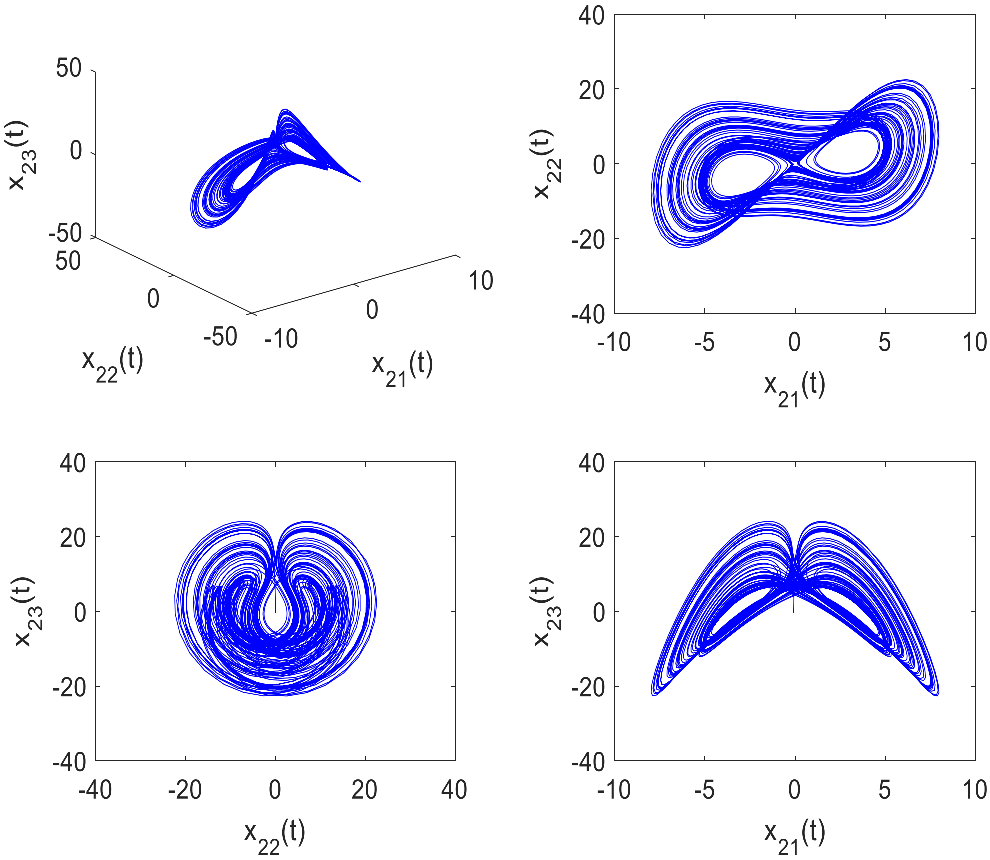

Fig. 3.5 Chaotic attractors of 3D chaotic system without exponential term for the values of the parameters $a_{21} = 0.8696$, $a_{22} = 0.5$, $a_{23} = 10.5$, $k = 0.756144$ and initial condition $(x_{21}, x_{22}, x_{23}) = (-0.08, -1.02, -0.49)$.

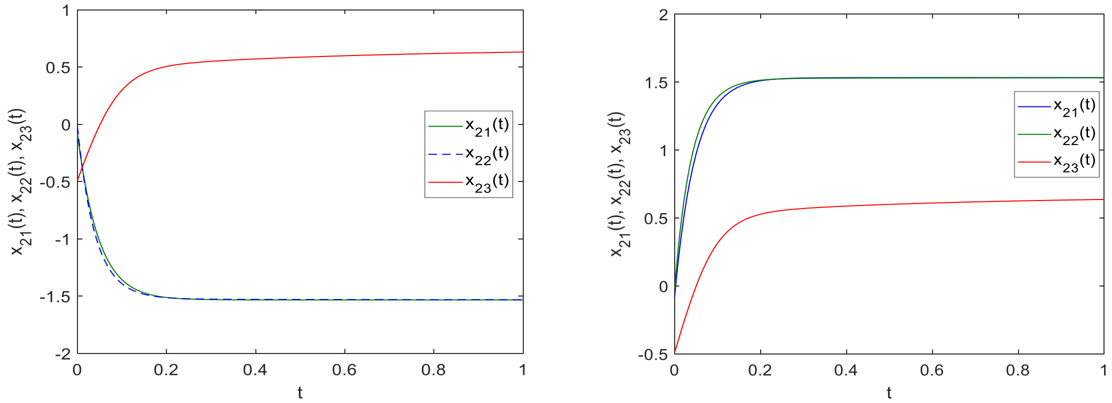

(a) (b)

Fig. 3.6 Chaos control of the 3D chaotic system (a) at the equilibrium point E_{21}, (b) at the equilibrium point E_{22}.

3.4.3 New 3D chaotic system

The new 3D chaotic system (Wei and Yang (2011)) is defined by equation (3.19) as

$$\frac{dx_{31}}{dt} = x_{32} - x_{31},$$

$$\frac{dx_{32}}{dt} = x_{31}x_{33} + a_{31}, \qquad (3.19)$$

$$\frac{dx_{33}}{dt} = \mu - e^{x_{31}x_{32}},$$

where x_{31}, x_{32}, x_{33} are the state variables of the system (3.19), μ is the real constant and a_{31} is the constant control parameter. The system is chaotic for a wide range of parameters and has interesting dynamic behaviors. If we take $\mu = 5$ and $a_{31} = 2$ with the initial condition $(1, 2, 3)$, the system shows chaotic behavior which is depicted through Figs. 3.7 and the Lyapunov exponent is 0.1442, 0.0002, -1.1445 which shows that the system is chaotic. If $\mu = 5$ and $a_{31} = 0$ with the same initial condition, the system is chaotic and displays a double scroll chaotic attractors with novel Lorenz-unlike or

Colpitts-unlike shaped, as depicted in Fig. 3.8 and the Lyapunov exponent is 0.4609, 0.0001, -1.4610.

If we replace the term $e^{x_{31}x_{32}}$ by $x_{31}x_{32}$ in equation (3.19), then New 3D chaotic system is reduced into a classical chaotic system whose chaotic behaviors are depicted through Figs. 3.9 and 3.10 for the parametric values $\mu = 5$, $a_{31} = 2$ and $\mu = 5$, $a_{31} = 0$ respectively.

If $a_{31} = 0$, then it is easy to see that system (3.19) is invariant under the transformation $(x_{31}, x_{32}, x_{33}) \to (-x_{31}, -x_{32}, x_{33})$, i.e., the system has symmetry around the x_{33}-axis. For system (3.19), the divergence $\nabla.V = -1 < 0$, which shows that the system (3.19) is dissipative and the solutions of the system are bounded with time.

The equilibrium points of the system (3.19) will be obtained by solving the following system of equations as

$$x_{32} - x_{31} = 0,\ x_{31}x_{33} + a_{31} = 0,\ \mu - e^{x_{31}x_{32}} = 0.$$

If $\mu > 1$, the system has two equilibrium points as

$$E_{31} = (\sqrt{\log(\mu)},\ \sqrt{\log(\mu)},\ -\frac{a_{31}}{\sqrt{\log(\mu)}}), \qquad E_{32} = (-\sqrt{\log(\mu)},\ -\sqrt{\log(\mu)},\ \frac{a_{31}}{\sqrt{\log(\mu)}})$$ or

$$E_{31} = (1.26864, 1.26864, -1.57650),\ E_{32} = (-1.26864, -1.26864, 1.57650).$$

Table 3.3 Lyapunov exponents for the New 3D chaotic system

Sl. No.	Initial Condition	Observation Time (T)	Lyapunov Exponents
A. For the parameters' values $\mu = 5$ and $a_{31} = 2$			
1	1, 4, 5	10000	0.1556, 0.0001, -1.1558
2	2, 5, 3	10000	0.1443, -0.0218, -1.1225
3	0.5, 0.1, 3	10000	0.1496, 0.0000, -1.1495
4	-1, -0.8, -2	10000	0.1531, 0.0000, -1.1531
B. For the parameters' values $\mu = 5$ and $a_{31} = 0$			
1	1, 4, 5	10000	0.4664, 0.0002, -1.4667
2	2, 5, 3	10000	0.4292, 0.0000, -1.4294
3	0.5, 0.1, 3	10000	0.4611, 0.0000, -1.4610
4	-1, -0.8, -2	10000	0.4629, 0.0001, -1.4630

3.4.3.1 Control of chaos

Consider the new 3D chaotic system with control function as

$$\frac{dx_{31}}{dt} = x_{32} - x_{31} + u_{31}(t),$$

$$\frac{dx_{32}}{dt} = x_{31}x_{33} + a_{31} + u_{32}(t), \tag{3.20}$$

$$\frac{dx_{33}}{dt} = \mu - e^{x_{31}x_{32}} + u_{33}(t),$$

where $u_{31}(t) = k_{31}(x_{31} - \bar{x}_{31})$, $u_{32}(t) = k_{32}(x_{32} - \bar{x}_{32})$, $u_{33}(t) = k_{33}(x_{33} - \bar{x}_{33})$ are control functions and k_{31}, k_{32}, k_{33} are the feedback controllers. The controlled system (3.20) can be rewritten as

$$\frac{dx_{31}}{dt} = x_{32} - x_{31} + k_{31}(x_{31} - \bar{x}_{31}),$$

$$\frac{dx_{32}}{dt} = x_{31}x_{33} + a_{31} + k_{32}(x_{32} - \bar{x}_{32}), \tag{3.21}$$

$$\frac{dx_{33}}{dt} = \mu - e^{x_{31}x_{32}} + k_{33}(x_{33} - \bar{x}_{33}) .$$

At the equilibrium point $E_3 = (\bar{x}_{31}, \bar{x}_{32}, \bar{x}_{33})$, the Jacobian matrix of the system (3.21) will be

$$J_3(E_3) = \begin{bmatrix} -1+k_{31} & 1 & 0 \\ \bar{x}_{33} & k_{32} & \bar{x}_{31} \\ -\bar{x}_{32}e^{\bar{x}_{31}\bar{x}_{32}} & -\bar{x}_{31}e^{\bar{x}_{31}\bar{x}_{32}} & k_{33} \end{bmatrix}.$$

Lemma 3.4: The equilibrium point $E_{31} = (\sqrt{\log(\mu)}, \sqrt{\log(\mu)}, -\frac{a_{31}}{\sqrt{\log(\mu)}})$ or $E_{31} = (p_2, p_2, -r_2)$, where $p_2 = \sqrt{\log(\mu)}$ and $r_2 = \frac{a_{31}}{\sqrt{\log(\mu)}}$ of the controlled system (3.21) is asymptotically stable if $k_{31} < 0$, $k_{32} < 0$, $k_{33} < 0$.

Proof: The Jacobian matrix of the controlled system (3.21) at the equilibrium point E_{31} is

$$J_{31}(E_{31}) = \begin{bmatrix} -1+k_{31} & 1 & 0 \\ -r_2 & k_{32} & p_2 \\ -p_2e^{p_2^2} & -p_2e^{p_2^2} & k_{33} \end{bmatrix}. \tag{3.22}$$

The characteristic polynomial of the Jacobian matrix (3.22) is

$$\lambda^3 + (1-k_{31}-k_{32}-k_{33})\lambda^2 + \{-k_{32} + k_{31}k_{32} + r_2 - k_{33}(1-k_{31}-k_{32}) + p_2^2e^{p_2^2})\}\lambda$$

$$-k_{33}(-k_{32} + k_{31}k_{32} + r_2) + 2p_2^2e^{p_2^2} - k_{32}p_2^2e^{p_2^2} = 0.$$

If we take $a_1 = 1-k_{31}-k_{32}-k_{33}$, $a_2 = -k_{32} + k_{31}k_{32} + r_2 - k_{33}(1-k_{31}-k_{32}) + p_2^2e^{p_2^2})$, $a_3 = -k_{33}(-k_{32} + k_{31}k_{32} + r_2) + 2p_2^2e^{p_2^2} - k_{32}p_2^2e^{p_2^2}$, then the characteristic polynomial is reduced in the form $\lambda^3 + a_1\lambda^2 + a_2\lambda + a_3 = 0$.

In the view of the Routh-Hurwitz condition (ii), if we consider $k_{31} < 0$, $k_{32} < 0$, $k_{33} < 0$, the controlled system (21) will be asymptotically stable at the point E_{31}.

Similarly, the equilibrium point $E_{32} = (-\sqrt{\log(\mu)}, -\sqrt{\log(\mu)}, \frac{a_{31}}{\sqrt{\log(\mu)}})$ or $E_{32} = (-p_2, -p_2, r_2)$ of the system (3.19) is asymptotically stable if we choose the feedback controllers as $k_{31} < 0$, $k_{32} < 0$, $k_{33} < 0$.

The unstable trajectories of new 3D chaotic system are controlled at its equilibrium points, and the plots of trajectories of the system (3.20) are given in Figs. 3.11 (a)-(c).

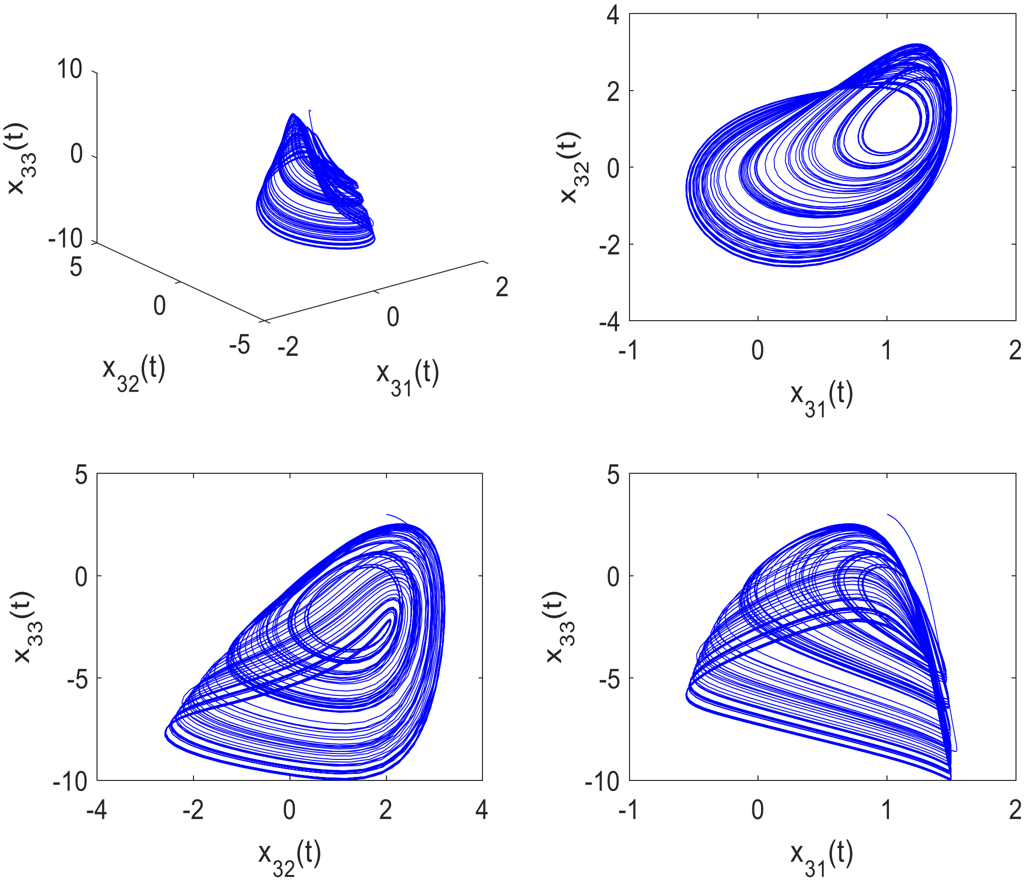

Fig. 3.7 Chaotic attractors of New 3D chaotic system with exponential term when $a_{31} = 2$ and initial condition $(1, 2, 3)$.

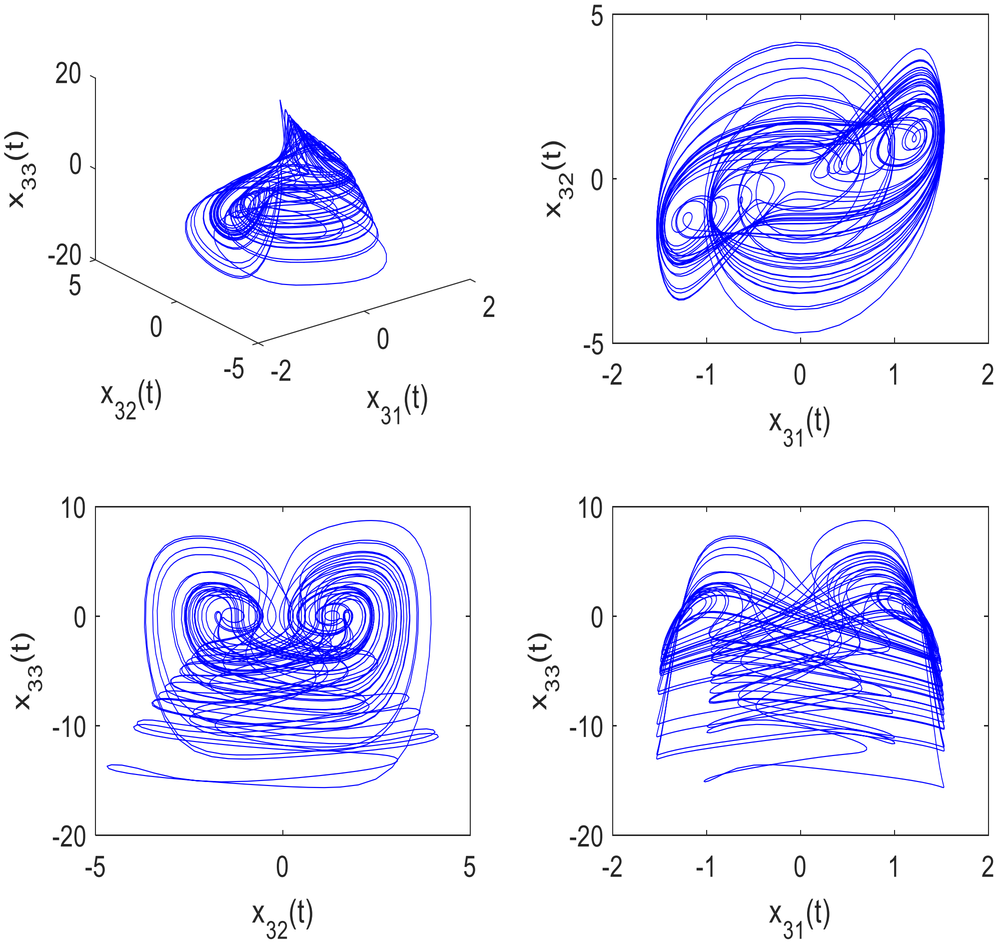

Fig. 3.8 Chaotic attractors of New 3D chaotic system with exponential term when $a_{31} = 0$ and initial condition $(1, 2, 3)$.

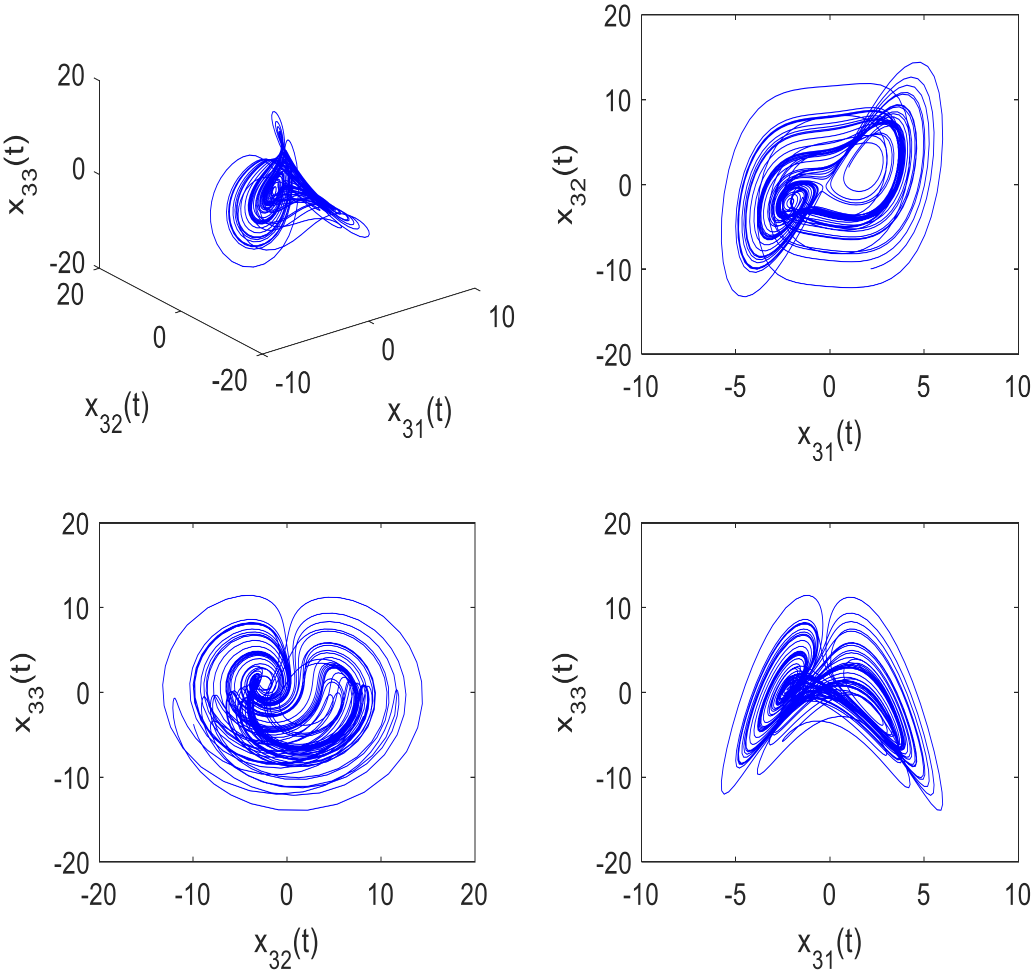

Fig. 3.9 Chaotic attractors of New 3D chaotic system without exponential term when $a_{31}=2$ and initial condition $(1, 2, 3)$.

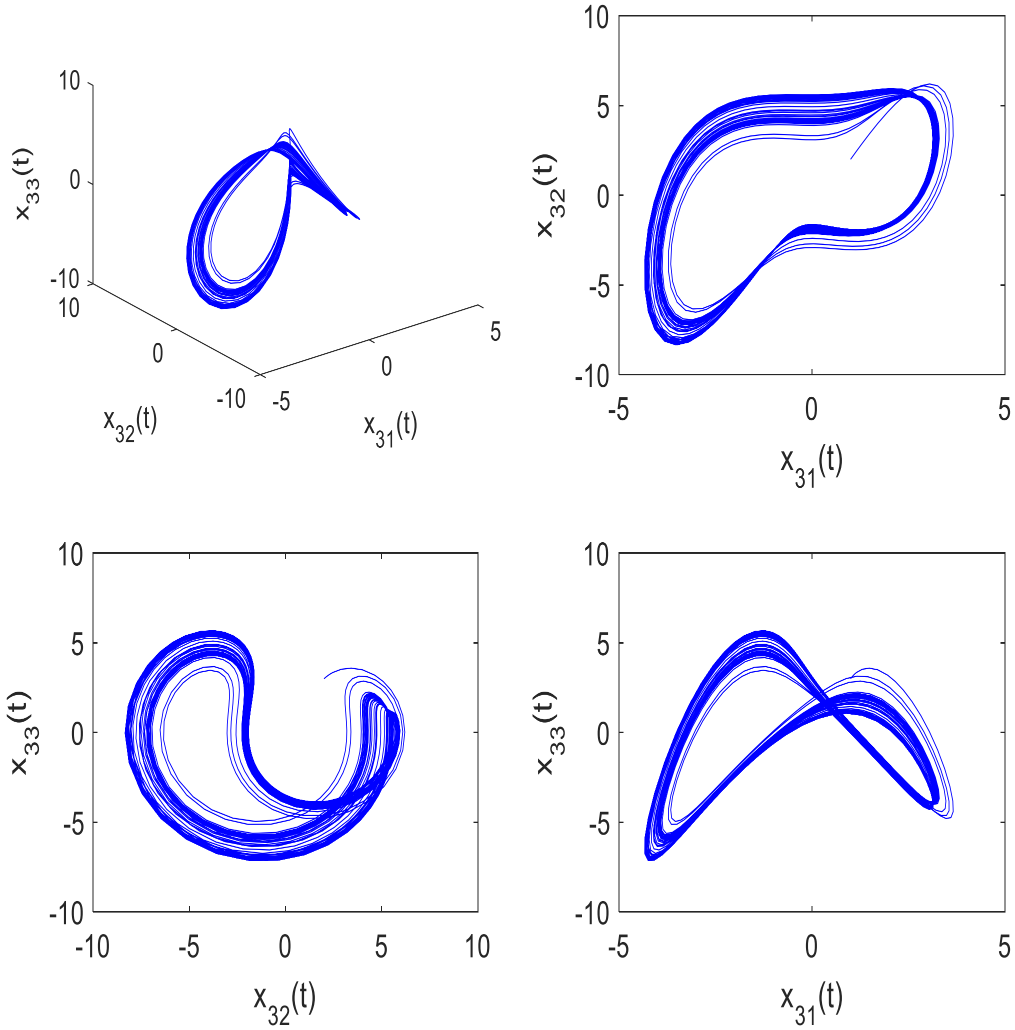

Fig. 3.10 Chaotic attractors of New 3D chaotic system without exponential term when $a_{31} = 0$ and initial condition $(1, 2, 3)$.

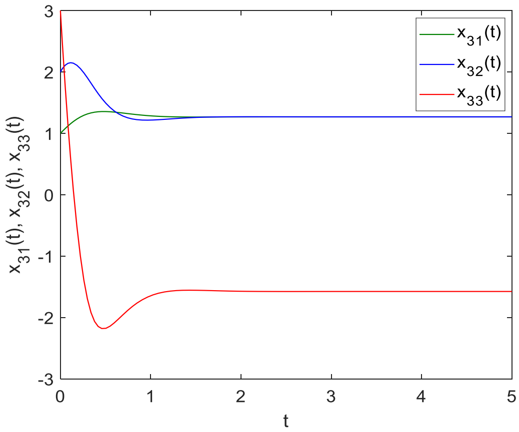

(a)

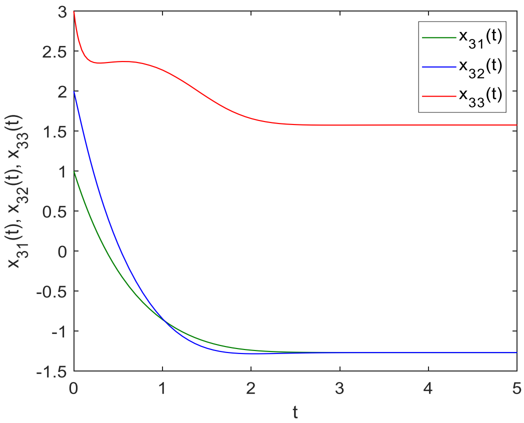

(b)

Fig. 3.11 Chaos control of New 3D chaotic system: (a) at the equilibrium point E_{31}, (b) at the equilibrium point E_{32}.

3.5 Application of difference synchronization scheme among chaotic systems

In this section, we will study the difference synchronization among continuous time chaotic systems with and without exponential terms, and also among discrete time chaotic systems.

3.5.1 Difference synchronization among chaotic systems with exponential terms

To study the difference synchronization among the chaotic systems in the presence of exponential terms, let us consider the Ten-ring chaotic system (3.8) and 3D chaotic system (3.14) as two master systems and the slave system as the system (3.19) with control functions as

$$\begin{aligned}
\frac{dx_{31}}{dt} &= x_{32} - x_{31} + u_1(t), \\
\frac{dx_{32}}{dt} &= x_{31}x_{33} + a_{31} + u_2(t), \qquad (3.23)\\
\frac{dx_{33}}{dt} &= \mu - e^{x_{31}x_{32}} + u_3(t),
\end{aligned}$$

where $u_1(t)$, $u_2(t)$ and $u_3(t)$ are the controllers, and it will be designed using feedback control technique. The error functions among two master and one slave systems are defined as

$$e_1 = l_{31}x_{31} - l_{21}x_{21} + l_{11}x_{11},$$

$$e_2 = l_{32}x_{32} - l_{22}x_{22} + l_{12}x_{12}, \tag{3.24}$$

$$e_3 = l_{33}x_{33} - l_{23}x_{23} + l_{13}x_{13},$$

where $L_3 = diag(l_{31},\, l_{32},\, l_{33}) \neq 0$, $L_2 = diag(l_{21},\, l_{22},\, l_{23})$ and $L_1 = diag(l_{11},\, l_{12},\, l_{13})$ are the constant matrices. The derivative of equation (3.24) is given as

$$\frac{de_i}{dt} = l_{3i}\frac{dx_{3i}}{dt} - l_{2i}\frac{dx_{2i}}{dt} + l_{1i}\frac{dx_{1i}}{dt},\ i = 1,2,3. \tag{3.25}$$

Using equations (3.8), (3.14), (3.23) and (3.25), we obtain the following error system as

$$\frac{de_1}{dt} = -e_1 + \frac{l_{31}}{l_{32}}e_2 + (\frac{l_{31}}{l_{32}}l_{22} - l_{21}a_{21})x_{22} + (a_{11}l_{11} - \frac{l_{31}l_{12}}{l_{32}})x_{12} + l_{21}(a_{21}-1)x_{21} + l_{11}(a_{11}+1)x_{11} + l_{31}u_1(t)$$

$$\tag{3.26}$$

$$\frac{de_2}{dt} = e_2 - l_{32}x_{32} + l_{22}(a_{22}+1)x_{22} - l_{12}(a_{13}+1)x_{12} + l_{32}x_{31}x_{33} - kl_{22}x_{21}x_{23} - l_{12}x_{11}x_{13} + a_{14}l_{12}x_{11} + l_{32}a_{31} + l_{32}u_2(t)$$

$$\frac{de_3}{dt} = e_3 - l_{33}x_{33} + l_{23}x_{23} - l_{13}(a_{12}+1)x_{13} + l_{33}\mu - l_{23}a_{23} - l_{33}e^{x_{31}x_{32}} + l_{23}e^{x_{21}x_{22}} + l_{13}e^{x_{11}^2} + l_{33}u_3(t).$$

Theorem 3.1: If the control functions are taken as

$$u_1(t) = \frac{1}{l_{31}}\{-k_1e_1 - (\frac{l_{31}}{l_{32}}l_{22} - l_{21}a_{21})x_{22} - (a_{11}l_{11} - \frac{l_{31}l_{12}}{l_{32}})x_{12} - l_{21}(a_{21}-1)x_{21} - l_{11}(a_{11}+1)x_{11}\}$$

$$u_2(t) = \frac{1}{l_{32}}\{-k_2e_2 + l_{32}x_{32} - l_{22}(a_{22}+1)x_{22} + l_{12}(a_{13}+1)x_{12} - l_{32}x_{31}x_{33} + kl_{22}x_{21}x_{23} + l_{12}x_{11}x_{13} - a_{14}l_{12}x_{11} - l_{32}a_{31}\}$$

(3.27)

$$u_3(t) = \frac{1}{l_{33}}\{-k_3e_3 + l_{33}x_{33} - l_{23}x_{23} + l_{13}(a_{12}+1)x_{13} - l_{33}\mu + l_{23}a_{23} + l_{33}e^{x_{31}x_{32}} - l_{23}e^{x_{21}x_{22}} - l_{13}e^{x_{11}^2}\},$$

and the feedback controllers are chosen as $k_1 > -1$, $k_2 > 1$, $k_3 > 1$, then the considered systems (3.8), (3.14) and (3.23) will be difference synchronized.

Proof: After putting the values of control functions from equation (3.27) in the error system (3.26), the error system is reduced to

$$\frac{de_1}{dt} = -(k_1+1)e_1 + \frac{l_{31}}{l_{32}}e_2,$$

$$\frac{de_2}{dt} = (1-k_2)e_2, \qquad (3.28)$$

$$\frac{de_3}{dt} = (1-k_3)e_3.$$

The Jacobian matrix of the system (3.28) is

$$J = \begin{bmatrix} -(k_1+1) & \frac{l_{31}}{l_{32}} & 0 \\ 0 & (1-k_2) & 0 \\ 0 & 0 & (1-k_3) \end{bmatrix}. \qquad (3.29)$$

The eigenvalues of the Jacobian matrix (3.29) are $\lambda_1 = -(k_1+1)$, $\lambda_2 = 1-k_2$ and $\lambda_3 = 1-k_3$, where k_1, k_2, k_3 are the feedback controllers. If we choose the feedback controllers as $k_1 > -1$, $k_2 > 1$, $k_3 > 1$, then the eigenvalues of the Jacobian matrix will be negative, and thus the error system (3.26) will be stabilized and the difference synchronization among considered chaotic systems with exponential terms will be achieved.

Remark IV: Now we will show the difference synchronization among chaotic systems without exponential terms and after putting the values of x_{11}^2 , $x_{21}x_{22}$, $x_{31}x_{32}$ in the place of $e^{x_{11}^2}$, $e^{x_{21}x_{22}}$, $e^{x_{31}x_{32}}$ of the chaotic systems (3.8), (3.14) and (3.19) respectively, the systems are reduced into a classical chaotic systems. Putting the above values in third equation $\frac{de_3}{dt}$ of error system (3.26), and control function $u_3(t)$ of equation (3.27), the equations $\frac{de_3}{dt}$ and $u_3(t)$ are reduced to the following forms:

$$\frac{de_3}{dt} = e_3 - l_{33}x_{33} + l_{23}x_{23} - l_{13}(a_{12}+1)x_{13} + l_{33}\mu - l_{23}a_{23} - l_{33}x_{31}x_{32} + l_{23}x_{21}x_{22} + l_{13}x_{11}^2 + l_{33}u_3(t),$$

$$u_3(t) = \frac{1}{l_{33}}\{-k_3e_3 + l_{33}x_{33} - l_{23}x_{23} + l_{13}(a_{12}+1)x_{13} - l_{33}\mu + l_{23}a_{23} + l_{33}x_{31}x_{32} - l_{23}x_{21}x_{22} - l_{13}x_{11}^2\}.$$

Following the same procedure like Theorem 3.1, the reduced classical chaotic systems will be synchronized.

3.5.2 Difference synchronization among discrete time chaotic systems

In this section we will study the difference synchronization among discrete time chaotic systems.

For difference synchronization, two master systems are considered as

$$X_1(n+1) = A_1X_1(n) + F_1(X_1(n)), \tag{3.30}$$

$$X_2(n+1) = A_2X_2(n) + F_2(X_2(n)), \tag{3.31}$$

and one slave system as

$$X_3(n+1) = A_3X_3(n) + F_3(X_3(n)) + U, \tag{3.32}$$

where $X_1(n), X_2(n), X_3(n) \in R^n$ are the state of the considered two master and one slave systems, respectively. $A_1, A_2, A_3 \in R^{n\times n}$ are the matrices, which are the coefficient of linear parts of the state variables, $F_1, F_2, F_3 : R^n \to R^n$ are the nonlinear parts of the systems and U is the control function which will be designed later during synchronization with the help of control technique.

Now, we define the error function as

$$e(n) = L_3 X_3(n) - L_2 X_2(n) + L_2 X_1(n). \tag{3.33}$$

Theorem 3.2 (Ouannas et al. (2018)**):** The considered two master systems (3.30) and (3.31) and one slave system (3.32) are said to be difference synchronized if the controller is taken as

$U = -A_3 X_3(n) - F_3(X_3(n)) + L_3^{-1}[-R]$, and

$$R = (L - A_3)e(n) - L_2[A_2 X_2(n) + F_2(X_2(n))] + L_1[A_1 X_1(n) + F_1(X_1(n))],$$

where $L \in R^{n\times n}$ is constant matrix and chosen in such a way that the eigenvalues of the matrix $(A_3 - L)$ are placed strictly inside the unit disk.

Proof: According to definition 3.1 of difference synchronization and from equations (3.30)-(3.33), the error systems can be derived as

$$e(n+1) = (A_3 - L)e(n) + L_3[A_3 X_3(n) + F_3(X_3(n)) + U] + R. \tag{3.34}$$

After putting the value of the control function U in equation (3.34), the error system is reduced in the following form

$$e(n+1) = (A_3 - L)e(n). \tag{3.35}$$

If the eigenvalues of the matrix $(A_3 - L)$ are placed strictly inside the unit disk, then from the asymptotic stability theory of linear discrete time dynamical systems, all the solutions of error system (3.35) tend to zero as $n \to \infty$. Hence, the considered master systems (3.30) and (3.31), and the slave system (3.32) are difference synchronized.

Now to demonstrate the difference synchronization we will consider the Wang and 3D Henon map discrete time systems (Ouannas et al. (2018), Yan (2006)) as the master systems I and II and the discrete time Rossler system as slave system.

The Wang system is given by

$$x_{11}(n+1) = a_{13}\delta\, x_{12}(n) + (a_{14}\delta + 1)x_{11}(n),$$

$$x_{12}(n+1) = a_{12}\delta\, x_{13}(n) + a_{11}\delta\, x_{11}(n) + x_{12}(n), \tag{3.36}$$

$$x_{13}(n+1) = a_{15}\delta + a_{6}\delta\, x_{12}(n)x_{13}(n) + (a_{17}\delta + 1)x_{13}(n).$$

The system (3.36) shows chaotic behavior for the parameters' values $a_{11} = -1.9$, $a_{12} = 0.2$, $a_{13} = 0.5$, $a_{14} = -2.3$, $a_{15} = 2$, $a_{16} = -0.6$, $a_{17} = -1.9$, $\delta = 1$ and initial condition $(x_{11}(0),\, x_{12}(0),\, x_{13}(0)) = (0.1,\, 0.2,\, 0.2)$, which is depicted through Fig. 3.14(a).

Comparing equation (3.30) and (3.36), we get

$$A_1 = \begin{bmatrix} (a_{14}\delta + 1) & a_{13}\delta & 0 \\ a_{11}\delta & 1 & a_{12}\delta \\ 0 & 0 & (a_{17}\delta + 1) \end{bmatrix}, \quad F_1(X_1(n)) = \begin{bmatrix} 0 \\ 0 \\ a_{15}\delta + a_{6}\delta\, x_{12}(n)x_{13}(n) \end{bmatrix}.$$

The 3D Henon map is defined as

$$x_{21}(n+1) = -a_{22}x_{22}(n),$$

$$x_{22}(n+1) = x_{23}(n) + 1 - a_{21}\, x_{22}^{2}(n), \tag{3.37}$$

$$x_{23}(n+1) = a_{22}x_{22}(n) + x_{21}(n).$$

At the parameters' values $a_{21} = 1.07$, $a_{12} = 0.3$ and initial condition $(x_{21}(0),\ x_{22}(0),\ x_{23}(0)) = (0.3,\ 0.5,\ 0.5)$, the system (3.37) shows the chaotic behavior and it is depicted through the Fig. 3.14(b).

In the view of equations (3.31) and (3.37), we get

$$A_2 = \begin{bmatrix} 0 & -a_{22} & 0 \\ 0 & 0 & 1 \\ 1 & a_{22} & 0 \end{bmatrix},\quad F_2(X_2(n)) = \begin{bmatrix} 0 \\ 1 - a_{21}\, x_{22}^2(n) \\ 0 \end{bmatrix}.$$

The discrete time Rossler system (Singh and Roy (2016)) with control functions is defined as

$$\begin{aligned} x_{31}(n+1) &= a_{31}x_{31}(n)(1 - x_{31}(n)) - a_{32}(x_{33}(n) + a_{33})(1 - 2x_{32}(n)) + u_1, \\ x_{32}(n+1) &= a_{34}x_{32}(n)(1 - x_{32}(n)) + a_{35}x_{33}(n) + u_2, \\ x_{33}(n+1) &= a_{36}((x_{33}(n) + a_{33})(1 - 2x_{32}(n)) - 1)(1 - a_{37}x_{31}(n)) + u_3. \end{aligned} \tag{3.38}$$

The system (3.38) shows chaotic behavior for the parameters values $a_{31} = 3.8$, $a_{32} = 0.05$, $a_{33} = 0.35$, $a_{34} = 3.78$, $a_{35} = 0.2$, $a_{36} = 0.1$, $a_{37} = 1.9$ with initial condition $(x_{31}(0),\ x_{32}(0),\ x_{33}(0)) = (0.1,\ 0.1,\ 0)$ which is displayed through Fig. 3.14(c).

Now comparing the equation (3.32) and (3.38), we get

$$A_3 = \begin{bmatrix} a_{31} & 2a_{32}a_{33} & -a_{32} \\ 0 & a_{34} & a_{35} \\ a_{36}a_{37}(1 - a_{33}) & -2a_{36}a_{33} & a_{36} \end{bmatrix},$$

$$F_3(X_3(n)) = \begin{bmatrix} -a_{31}x_{31}^2(n) + 2a_{32}x_{32}x_{33} - a_{32}a_{33} \\ -a_{34}\, x_{32}^2(n) + a_{35}x_{33}(n) \\ a_{36}a_{33} - a_{36} - 2a_{36}x_{32}(n)x_{33}(n) - a_{36}a_{37}x_{31}(n)x_{33}(n) + 2a_{36}a_{37}x_{31}(n)x_{32}(n)x_{33}(n) \\ + 2a_{36}a_{37}a_{33}x_{31}(n)x_{32}(n) \end{bmatrix}.$$

Now choosing the matrix L as

$$L=\begin{bmatrix} 4 & 0.035 & -0.05 \\ 0 & 4 & 0.02 \\ 0.1235 & -0.07 & 1 \end{bmatrix},$$

the error systems with the aid of Theorem 3.2 , we get

$$\begin{aligned} e_1(n+1) &= (a_{34}-4)e_1(n)+(2a_{32}a_{33}-0.035)e_2(n)+(0.05-a_{32})e_3(n), \\ e_2(n+1) &= (a_{34}-4)e_2(n)+(a_{35}-0.02)e_3(n), \\ e_3(n+1) &= (a_{36}a_{37}(1-a_{33})-0.1235)e_1(n)+(0.07-2a_{36}a_{33})e_2(n)+(a_{36}-1)e_3(n). \end{aligned} \tag{3.39}$$

From equation (3.39), it is clear that the eigenvalues of the error systems are placed strictly inside the unit disk, and hence from the asymptotic stability theory of linear discrete time dynamical systems, the considered master systems (3.36) and (3.37), and slave system (3.38) will be difference synchronized.

3.6 Numerical simulation and discussion

In this section, during simulation of difference synchronization and chaos control of the systems, the earlier considered values of the parameters of chaotic systems are taken, and the initial conditions of Ten-ring chaotic system, 3D chaotic system, and new 3D chaotic system are taken as $(0.02, 0.01, 0.03)$, $(-0.08, -0.02, -0.49)$ and $(1, 2, 3)$ respectively. Thus according to the definition of error functions the initial condition of the error system will be $(1.88, 2.12, 3.99)$. Figs. 3.3(a)-(c) show that the Ten-ring chaotic system can be stabilized to its equilibrium points E_{11} and E_{12} as and when we choose the feedback controllers as $k_{11}<-a_{11}$, $k_{12}<a_{13}$, $k_{13}<a_{12}$ and $k_{11}<-a_{11}$, $k_{12}<0$, $k_{13}<0$. The chaos control of 3D chaotic system is performed by the Figs. 3.6(a)-(b), which is stable at its equilibrium points when taking the feedback controllers as $k_{21}<0$, $k_{22}<0$, $k_{23}<0$. Similarly the Figs. 3.11(a)-(b) describe that the new 3D chaotic system is stable at equilibrium points when we consider the feedback controllers as $k_{31} < 0$, $k_{32} < 0$, $k_{33} < 0$. The difference synchronization is demonstrated among the said chaotic systems with exponential terms using feedback control technique. The trajectories of master and slave systems are synchronized after a small time of duration which are shown through Figs. 3.12(a)-(c). The Fig. 3.12(d) describes that the error functions converge to zero when time becomes large which predicts that the systems are difference synchronized.

The difference synchronization among the chaotic systems with the first order approximations of the exponential terms i.e., among the classical systems using feedback control technique is presented through Fig. 3.13. The trajectories of master and slave systems are synchronized after a small time of duration which is also shown through Figs. 3.13(a)-(c). It is also clear from the Fig. 3.13(d) that the error functions converge to zero when time becomes large which clearly confirm the difference synchronization among the classical chaotic systems.

During demonstration of difference synchronization among discrete time chaotic systems, the earlier considered values of the parameters of systems with the initial conditions of Wang, 3D Henon Map and Rossler systems are taken. Thus according to the definition of error functions the initial condition of the error system will be $(-0.1, 0.2, -0.3)$. The synchronization among the said discrete time chaotic systems is graphically presented through Figs. 3.14(d)-(f) as the error functions converge to zero as $n \to \infty$. Hence, the considered master systems (3.36) and (3.37) are difference synchronized with the slave system (3.38).

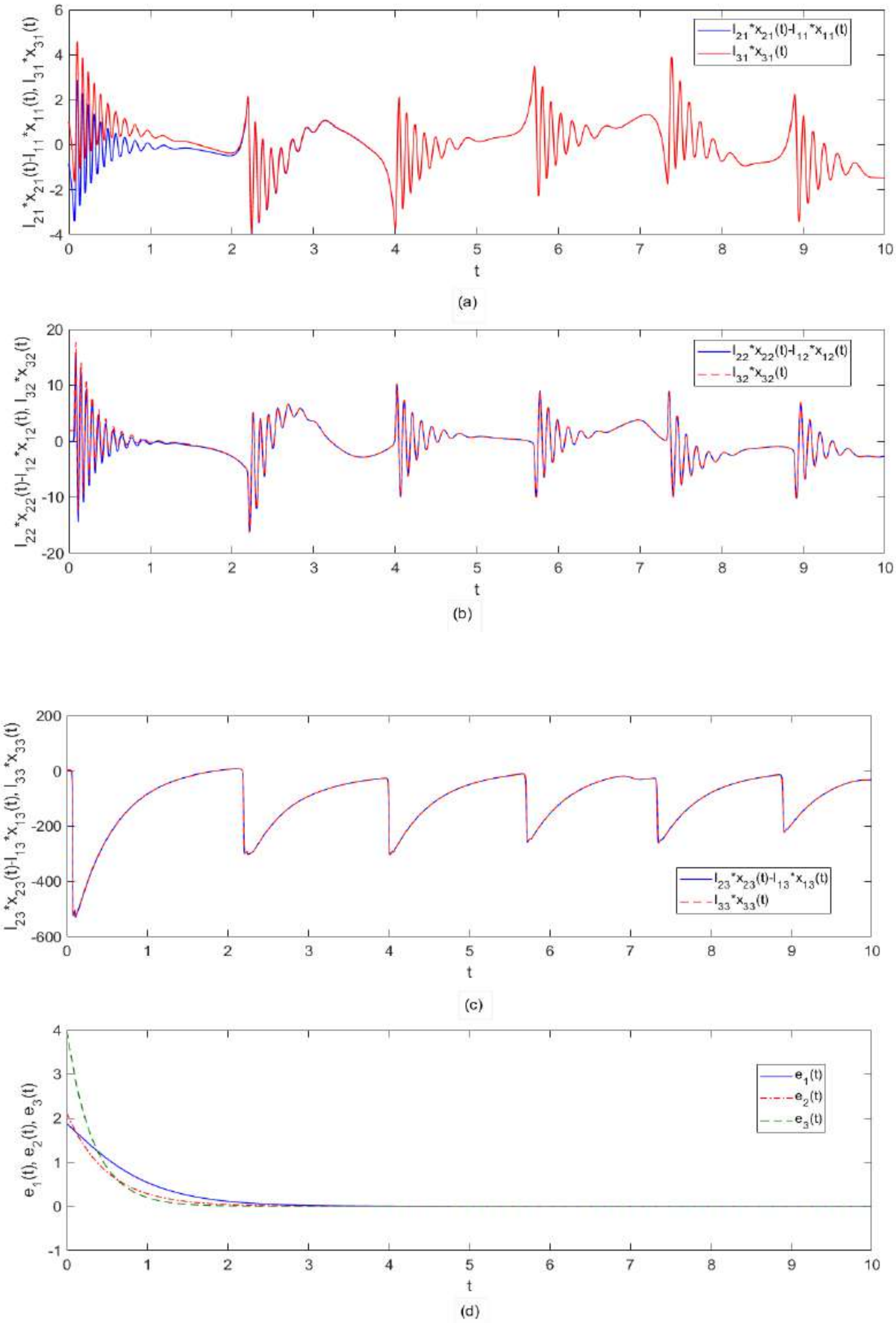

Fig. 3.12 State trajectories of difference synchronization among chaotic systems with exponential terms: (a) between $l_{21}x_{21} - l_{11}x_{11}$ and $l_{31}x_{31}$, (b) between $l_{22}x_{22} - l_{12}x_{12}$ and $l_{32}x_{32}$, (c) between $l_{23}x_{23} - l_{13}x_{13}$ and $l_{33}x_{33}$, (d) plots of error functions $e_1(t)$, $e_2(t)$ and $e_3(t)$.

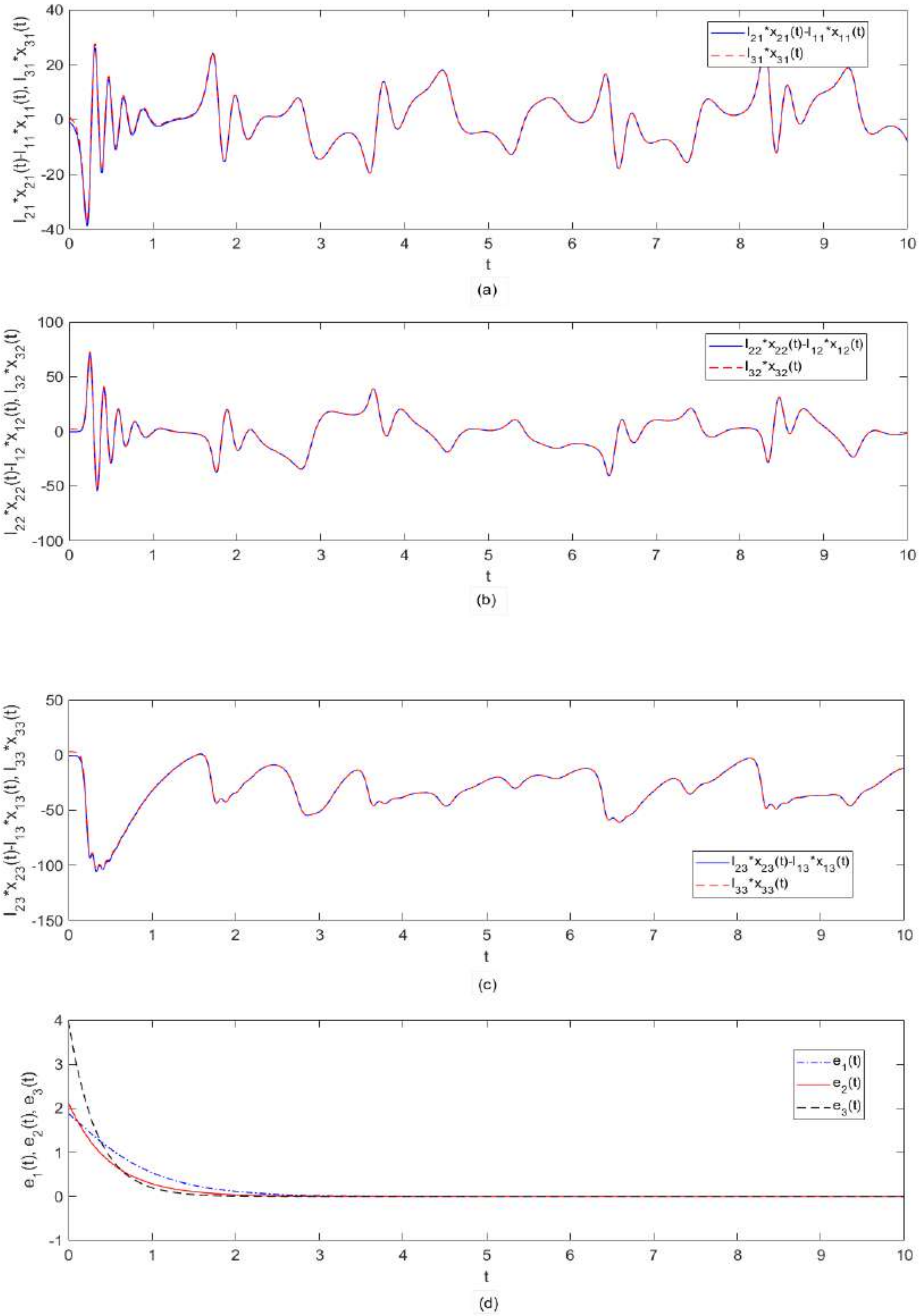

Fig. 3.13 State trajectories of difference synchronization among chaotic systems without exponential terms: (a) between $l_{21}x_{21} - l_{11}x_{11}$ and $l_{31}x_{31}$, (b) between $l_{22}x_{22} - l_{12}x_{12}$ and $l_{32}x_{32}$, (c) between $l_{23}x_{23} - l_{13}x_{13}$ and $l_{33}x_{33}$, (d) plots of error functions $e_1(t)$, $e_2(t)$ and $e_3(t)$.

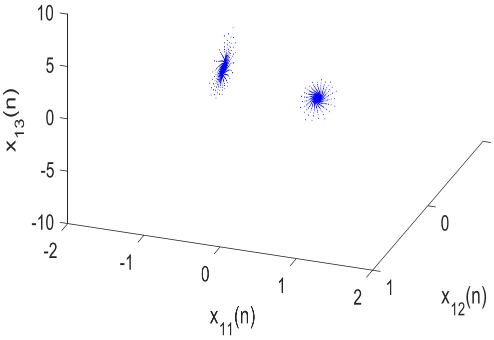
10
5
0
-5
-10
x13(n)
-2
-1
0
1
2
x11(n)
1
0
-1
x12(n)

(a)

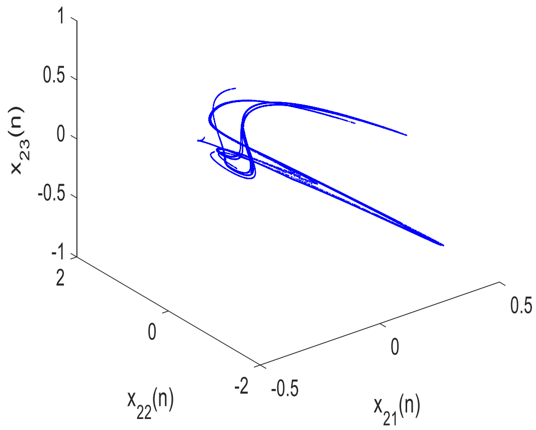
1
0.5
0
-0.5
-1
x23(n)
2
0
-2
x22(n)
-0.5
0
0.5
x21(n)

(b)

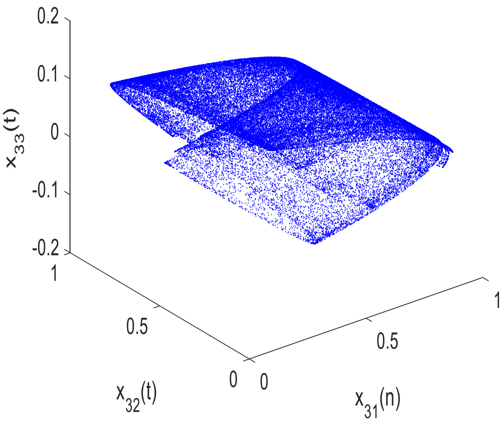
0.2
0.1
0
-0.1
-0.2
x33(t)
1
0.5
0
x32(t)
0
0.5
1
x31(n)

(c)

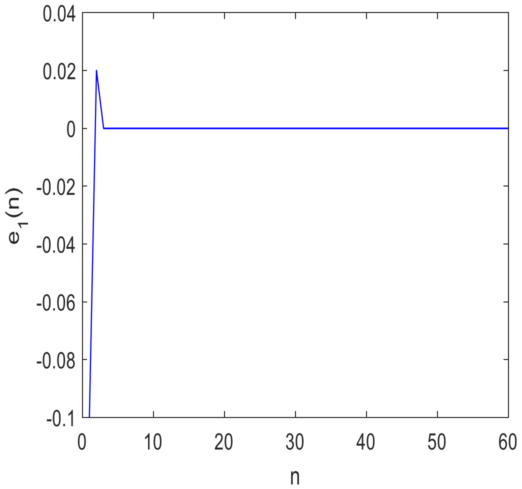
0.04
0.02
0
-0.02
-0.04
-0.06
-0.08
-0.1
e1(n)
0
10
20
30
40
50
60
n

(d)

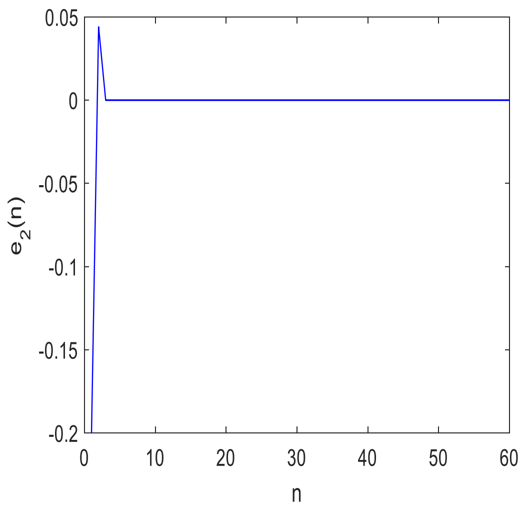

(e)

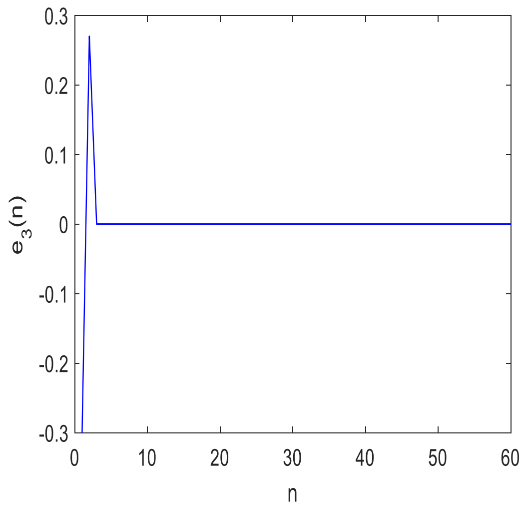

(f)

Fig. 3.14 (a) The chaotic attractors of discrete time Wang system; (b) The chaotic attractors of discrete time 3D Henon map; (c) The chaotic attractors of discrete time Rossler system; (d) Plot of error function $e_1(n)$ for difference synchronization; (e) Plot of error function $e_2(n)$ for difference synchronization; (f) Plot of error function $e_3(n)$ for difference synchronization.

3.7 Conclusion

In this chapter, the difference synchronization among Ten ring, 3D and new 3D chaotic systems with exponential terms and also for classical form of those systems with the chaos control have been studied using linear feedback control technique with the help of Routh-Hurwitz conditions.

The difference synchronization among discrete time chaotic systems has also been done using the asymptotic stability theory of linear discrete time systems. The chaos control of the considered systems at its equilibrium points has been studied by using linear feedback control, and it also observed that all three systems could be controlled to its equilibrium points. During difference synchronization, the controllers are designed systematically via feedback control method. The numerical simulations and graphical results demonstrate the validity of the difference synchronization technique. As a new type of synchronization technique was required in dynamical system towards improvement of information security, therefore a successful drive has been made to achieve the difference synchronization scheme to increase the security of the signals between transmitter and receiver through chaotic secure communication because of the complexity of the said technique. My future research will be focused on difference synchronization among chaotic systems with exponential terms in the presence of noise.

*****